

# EFFECT OF A RADIATION SHIELD ON THERMAL STRESS FIELD DURING CZOCHRALSKI CRYSTAL GROWTH OF SILICON

TAKAO TSUKADA AND MITSUNORI HOZAWA

Chemical Research Institute of Non-Aqueous Solutions,  
Tohoku University, Sendai 980

NOBUYUKI IMAISHI

Institute of Advanced Material Study,  
Kyushu University, Kasuga 816

**Key Words:** Crystal Growth, Silicon, Czochralski Method, Radiation Shield, Thermal Stress, Finite Element Method

For silicon CZ crystal growth, the effect of a radiation shield inserted in a furnace on the thermal stress field was studied theoretically by the finite-element method based on thermoelastic analysis.

It is found that a radiation shield lowers the maximum (thermally induced) shear stress, since it reduces the temperature gradient, especially in the radial direction, in a crystal. There is an optimum location for placement of the radiation shield so as to realize the smallest shear stress. From the viewpoint of thermal stress, a radiation shield can allow a higher pull rate of defect-free crystal.

## Introduction

Thermal stress induced by temperature variations during crystal growth is an important problem in the quality control of single crystals. If the local thermal stress exceeds the critical value, i.e. the yield stress, the crystal deforms plastically and dislocations occur.

A number of theoretical studies<sup>1-7,9-11)</sup> of thermal stress in crystals have been carried out, especially for GaAs single crystals. Some of them are based on assumptions of the flat melt/crystal interface or of planar strain. Since the interface shape is not flat and an axial temperature gradient exists in the crystal, the analyses based on the above assumptions seem insufficient. In the course of developing this paper, Lambropoulos *et al.*<sup>6)</sup> discussed the effect of interface shape on thermal stress. Their analysis was based on unrealistic thermal boundary conditions and modeled a parabolic interface shape.

Recently, the finite element method<sup>8)</sup> has been developed to predict temperature distribution and thermal stress field in a growing crystal with a curved melt/crystal interface.

We have reported our finite element analyses<sup>13,14)</sup> of a CZ puller. In these reports, temperature distributions in the melt and crystal and the effect of a radiation shield were discussed on the basis of our analyses, in which the shapes of melt/crystal and melt/gas interfaces along with the directed and reflected radiative heat transfer were taken into account. From the thermal point of view, it was found

that a radiation shield, placed at an appropriate position in the furnace, can (1) flatten the melt/crystal interface shape, (2) increase the pull rate and (3) reduce power consumption.<sup>13,14)</sup> But its effect on thermal stresses in the crystal rod was not discussed in the previous reports.

The aim of this work is to develop a thermal stress analysis by means of the finite element method based on thermoelastic analysis, and to investigate the effect of a radiation shield on the thermal stress field.

## 1. Theory

The thermal stress analysis by the finite element method in the present work is similar to that by the previous workers.<sup>2,7-10)</sup> Figure 1 shows the cylindrical coordinate system used here. The following assumptions are used in calculations. (1) The material is linearly elastic and isotropic. (2) The thermoelastic field is axisymmetric. (3) The body forces applied to the material are zero. (4) The crystal is free from

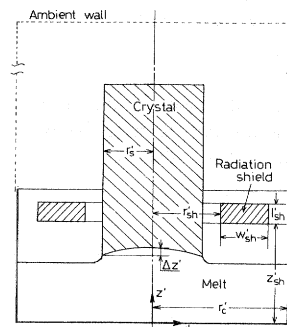


Fig. 1. Model of CZ crystal puller

\* Received April 17, 1989. Correspondence concerning this article should be addressed to T. Tsukada.

surface traction. (5) The mechanical properties are independent of temperature, although the temperature dependency can be easily incorporated into our calculation program.

The constitutive equation for linear elastic material in case of axisymmetry is expressed as follows.

$$\sigma = \begin{Bmatrix} \sigma_r \\ \sigma_z \\ \sigma_\theta \\ \tau_{rz} \end{Bmatrix} = \frac{E}{(1+\nu)(1-2\nu)} \begin{pmatrix} 1-\nu & \nu & \nu & 0 \\ & 1-\nu & \nu & 0 \\ & & 1-\nu & 0 \\ \text{sym.} & & & \frac{1-2\nu}{2} \end{pmatrix} \begin{Bmatrix} \varepsilon_r - \varepsilon_{r0} \\ \varepsilon_z - \varepsilon_{z0} \\ \varepsilon_\theta - \varepsilon_{\theta0} \\ \gamma_{rz} - \gamma_{rz0} \end{Bmatrix} \quad (1)$$

$$= D(\varepsilon - \varepsilon_0)$$

where  $E$  is Young's modulus and  $\nu$  is Poisson's ratio.  $\varepsilon_0$  is the initial strain which corresponds to free expansion or contraction caused by temperature variations and is given by Eq. (2).

$$\varepsilon_0 = \beta(T' - T_{ref}) \begin{Bmatrix} 1 \\ 1 \\ 1 \\ 0 \end{Bmatrix} \quad (2)$$

$T'$  is the local temperature in the crystal.

The strain-displacement equation is given by the following equation.

$$\varepsilon = \begin{pmatrix} \partial/\partial r & 0 \\ 0 & \partial/\partial z \\ 1/r & 0 \\ \partial/\partial z & \partial/\partial r \end{pmatrix} \begin{Bmatrix} u \\ v \end{Bmatrix} = Ad \quad (3)$$

The finite element method is applied to the thermal stress analysis, in which four-node quadrilateral elements are used. In each element, the displacement vector is approximated by

$$d = \phi a \quad (4)$$

where  $a$  is the nodal displacement vector.

Substituting Eq. (4) into Eq. (3), the strain is described by nodal displacements by Eq. (5).

$$\varepsilon = A\phi a = Ba \quad (5)$$

where  $B$  is the matrix derived from the derivatives of shape functions.

In the thermal stress analysis, the equilibrium equation and mechanical boundary conditions are necessary in addition to the above equations, and the

virtual work principle is applied in this calculation. Under the assumptions of (3) and (4), the virtual work principle gives the following equations.

$$\int_V \delta \varepsilon^T \sigma dV = 0 \quad (6)$$

Substituting Eqs. (1) and (5) into Eq. (6), the set of algebraic equations is given by Eq. (7).

$$\int_V B^T D B dV a = \int_V B^T D \varepsilon_0 dV \quad (7)$$

Eq. (7) is solved for nodal displacements under the boundary condition that the radial component of displacements is zero at the  $z$  axis.

Finally, the thermal stress field can be obtained by Eq. (8).

$$\sigma = D(Ba - \varepsilon_0) \quad (8)$$

A dislocation occurs in the crystal when the local stress exceeds the critical value, i.e. the yield stress. It is generally known that the shear stress is the most important factor in the initiation of a dislocation. Therefore, the maximum shear stress (Tresca stress), defined by Eq. (9), is used to present the final results of this analysis.

$$\tau_{max} = (\sigma_1 - \sigma_3)/2 \quad (9)$$

where  $\sigma_1$  and  $\sigma_3$  are principal stress ( $\sigma_1 > \sigma_2 > \sigma_3$ ).

## 2. Results and Discussion

We computed the thermal stress fields in the crystal during silicon CZ crystal growth with and without an annular radiation shield as shown in Fig. 1. The temperature distributions in the crystal obtained in our previous work<sup>14)</sup> were used in this thermal stress analysis. The mechanical properties, Young's modulus  $E$  and Poisson's ratio  $\nu$  were assumed to be constant,  $1.56 \times 10^5$  [MPa] and 0.25 respectively, because of the lack of reliable data for these properties dependent on temperature. Also, the linear expansion coefficient<sup>12)</sup> expressed by the following equation was used.

$$\beta = 1.887 \times 10^{-6} + 3.868 \times 10^{-9} T' - 13.632 \times 10^{-13} T'^2 \quad (10)$$

Physical properties and processing parameters are the same as in our previous work.<sup>13,14)</sup>

In the previous works,<sup>1-5,7,9-11)</sup> thermal stress in a cylindrical crystal with a flat melt/crystal interface was extensively analyzed. To investigate the effect of melt/crystal interface shape on the thermal stress field, a thermal stress analysis for the crystal with a flat interface was carried out, using the analytical solution of temperature distribution in the crystal expressed by Eq. (11), similarly to some previous

workers.<sup>1,3)</sup>

$$T = \sum_{n=1}^{\infty} A_n J_0(s_n r) \exp(-\alpha_n z) \quad (11)$$

where  $s_n$  is the  $n$ th root of  $sJ_1(s) - BiJ_0(s) = 0$

$$A_n = 2Bi / [(Bi^2 + s_n^2)J_0(s_n)]$$

$$\alpha_n = -Pe/2 + [(Pe/2)^2 + s_n^2]^{1/2}$$

In Eq. (11),  $Bi$  is the Biot number, defined by  $(hr'_s/k_l)$ , where the surface heat transfer coefficient  $h$  should be read as  $\varepsilon\sigma T_s'^3$  since radiation is dominant in the CZ system. In this work,  $Bi$  was assumed to be constant at the value evaluated at  $T'_s = T'_m$  regardless of the fact that  $T'_s$  (or  $Bi$ ) decreases rapidly with axial distance from the melt/crystal interface. **Figure 2** shows the isotherms (on the left) and isostress contours of  $\tau_{max}$  (maximum shear stresses) (on the right) in the crystal with flat melt/crystal interface. A relatively small  $\tau_{max}$  appears near the melt/crystal interface, especially near the contact line of three phases (melt, crystal and gas phases), because the melt/crystal interface shape is flat and thus the temperature gradient, especially in the radial direction, is small near the melt/crystal interface. The small thermal stress thus estimated near the interface is contradictory to the fact that, even in an industrial Si CZ puller, dislocation occasionally begins but only at a certain point near the three-phase contact line, although the mechanism is not yet well understood.

In our previous papers,<sup>13,14)</sup> the temperature distributions in the crystal were obtained by the finite element analysis based on the assumption of conduction dominant in the melt and crystal, taking non-flat melt/crystal and melt/gas interfaces into account. **Figure 3** shows isotherms then obtained and isostress contours of  $\tau_{max}$  in the crystal without a radiation shield at different stages of crystal growth, i.e. the different melt volumes (a)  $V_m = 0.23$  and (b)  $V_m = 0.125$ .  $\tau_{max}$  shows a maximum near the three-phase contact line corresponding to the steepest radial temperature gradient there. Figure 3 indicates that in order to estimate a thermal stress field in a crystal, the shape of the melt/crystal interface must be correctly taken into account.

**Figure 4** shows the radial distribution of  $\tau_{max}$  on the melt/crystal interface at various values of Peclet number  $Pe$ , nondimensional pull rate, without a radiation shield.  $\tau_{max}$  along the melt/crystal interface shows a minimum at  $r'/r'_s = 0.7-0.8$  and a maximum at the periphery of the crystal, and thus the distribution on the interface is W-shaped. This result can be explained from **Fig. 5**, which shows the distribution of normal strain in radial, axial and azimuthal directions on the melt/crystal interface. In **Fig. 5**, the sum of all strain components, i.e. total strain, has

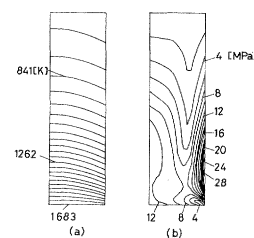


**Fig. 2.** Isotherms and isostress contours of maximum shear stress in a crystal with flat melt/crystal interface

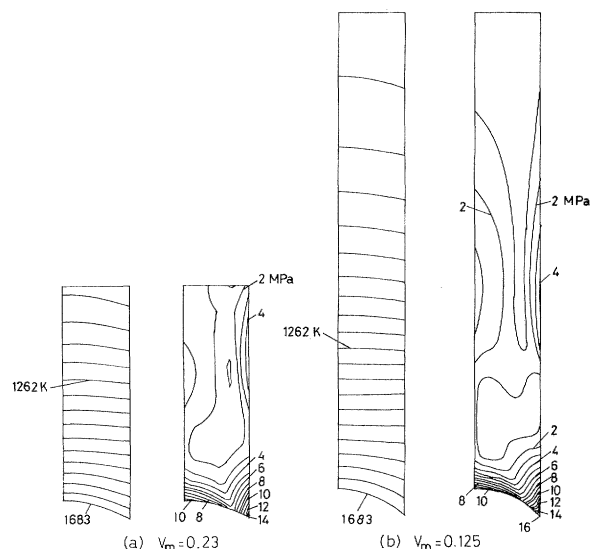


**Fig. 3.** Isotherms and isostress contours of maximum shear stress in a crystal without a radiation shield

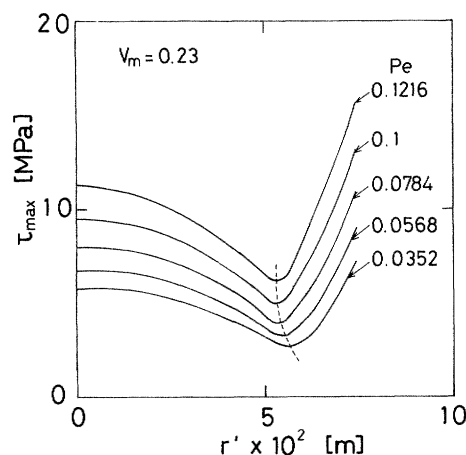


**Fig. 4.** Effect of  $Pe$  on the distribution of maximum shear stress on the melt/crystal interface without a radiation shield

minimum value at  $r'/r'_s = 0.7-0.8$ . Since the strain distribution is closely related to the stress distribution, thermal stress on the interface also shows minimum value at almost the same point. Figure 4 shows that the absolute value of shear stresses on the interface increases with  $Pe$ , and also that the location of the minimum value of shear stress shifts slightly inward as  $Pe$  increases.

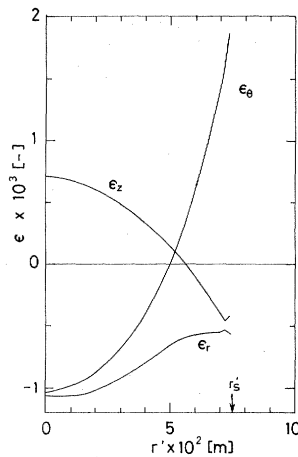


Fig. 5. Distribution of normal strain on the melt/crystal interface. ( $V_m=0.23$ ,  $Pe=0.1216$ )

These results suggest that the non-flat melt/crystal interface, which is convex to the crystal, causes large shear stress near the interface, and that generation of dislocation there becomes highly probable at very large pull rates. Therefore, there must exist an upper limit of pull rate to produce a dislocation-free single crystal. Accordingly, to reduce the thermal stress near the melt/crystal interface it is desirable to make the interface shape as flat as possible.

We reported in the previous work<sup>13,14)</sup> that a radiation shield inserted into the furnace is effective in reducing the arc height of the interface. In the following section, the effect of a radiation shield on the thermal stress field is investigated.

Figure 6 shows the isotherms and isostress contours of  $\tau_{max}$  in the crystal with a radiation shield as shown in Fig. 1, for (a)  $V_m=0.23$  and (b)  $V_m=0.125$ . An annular radiation shield with  $l_{sh}=0.15$ ,  $r_{sh}=0.5$  and  $w_{sh}=0.35$  is located at  $z_{sh}=0.65$  in Fig. 6(a), and at  $z_{sh}=0.5$  in Fig. 6(b). Compared with Fig. 3, it can be seen that with a radiation shield,  $\tau_{max}$  in the crystal, especially near the melt/crystal interface, is reduced by as much as 25–30%, because the melt/crystal interface becomes less convex to the crystal. The radial temperature gradient near the interface becomes smaller by insertion of the radiation shield.

Figure 7 shows the distribution of  $\tau_{max}$  on the melt/crystal interface at various  $z_{sh}$  values for (a)  $V_m=0.23$  and (b)  $V_m=0.125$ . In Fig. 7 the solid line shows the distribution with a radiation shield placed at various heights and the dotted line shows that without a shield. There exists an optimum value of  $z_{sh}$  at which the shear stresses on the melt/crystal interface become smallest.

Figure 8 shows the effect of  $z'_{sh}$  on  $\tau_{max}$  at the center axis ( $r=0$ ) and the periphery ( $r=r_s$ ) on the melt/crystal interface, for (a)  $V_m=0.23$  and (b)  $V_m=0.125$ . Figure 8 also shows the effects of  $z'_{sh}$  on the minimum value

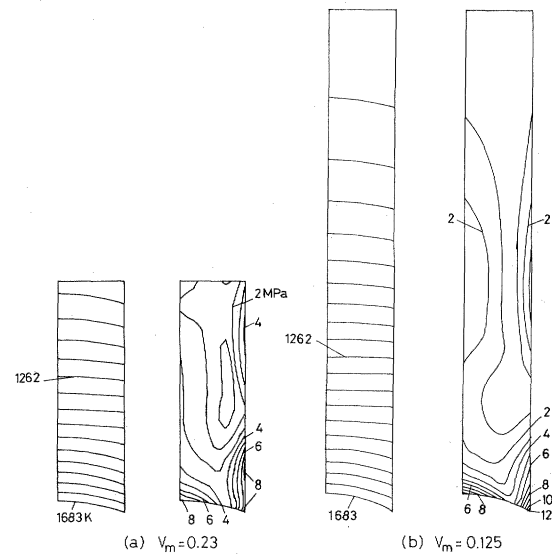


Fig. 6. Isotherms and isostress contours of maximum shear stress in a crystal with a radiation shield

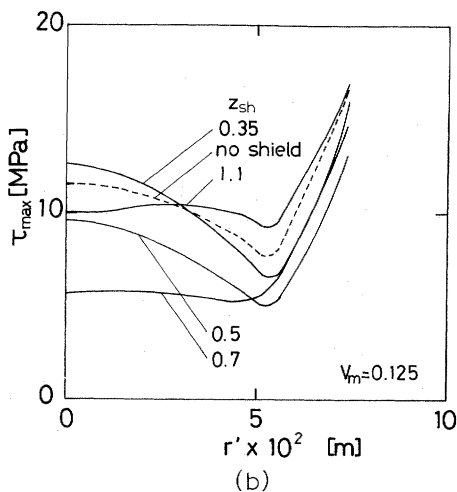
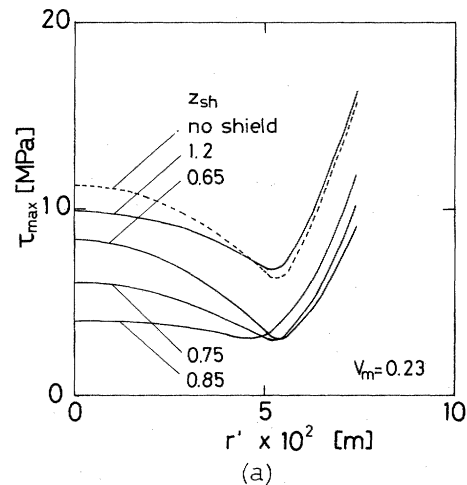


Fig. 7. Distribution of maximum shear stress on the melt/crystal interface at various  $z_{sh}$

of  $\tau_{max}$  on the interface, and on the maximum arc height of the interface,  $\Delta z'$ . For two melt volumes, the maximum shear stresses at both  $r=0$  and  $r=r_s$  have

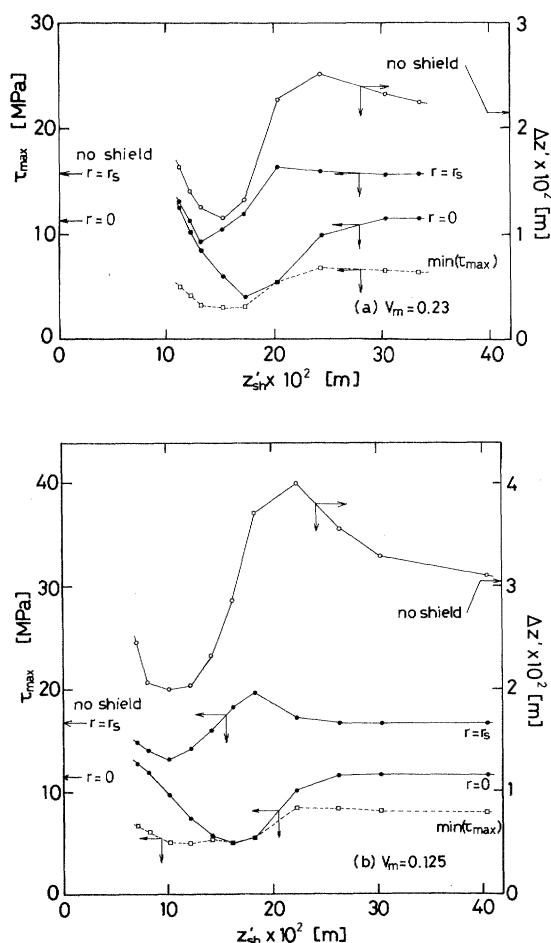


Fig. 8. Effect of  $z'_{sh}$  on maximum shear stress on the melt/crystal interface

minimum values at certain  $z'_{sh}$ ,  $z'_{sh}$ , corresponding to the smallest shear stress at the  $r=r_s$ , almost coincides with that corresponding to the smallest  $\Delta z'$ , while  $\tau_{max}$  at  $r=0$  shows its minimum at a slightly higher shield location.

Figure 9 shows the effect of Peclet number  $Pe$ , i.e. the pull rate, on the distribution of  $\tau_{max}$  on the melt/crystal interface. Apparently, the maximum shear stress becomes larger as  $Pe$  increases. The shear stress always shows a maximum at the periphery of the crystal. The radial position of the minimum shear stress shifts slightly inward as  $Pe$  increases. Compared with the results in Fig. 4, the maximum shear stress on the melt/crystal interface is considerably reduced by insertion of a radiation shield at any pull rate. In short, if there is a limited highest shear stress value to produce high quality crystal such as dislocation-free crystal, the pull rate with a radiation shield can be made higher than that without a shield, until maximum thermal stress value exceeds the limiting value.

In this work, the condition for generation of dislocation in the crystal could not be studied quantitatively, due to the lack of reliable data and

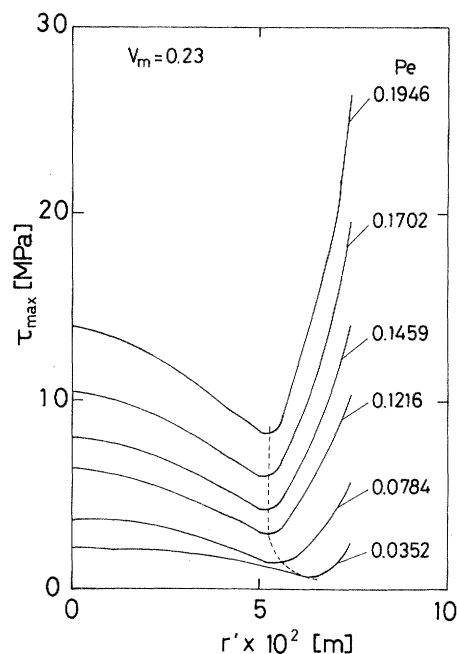


Fig. 9. Effect of  $Pe$  on distribution of maximum shear stress on the melt/crystal interface with a radiation shield

knowledge both of the yield stress of silicon at high, near melting, temperature and of the mechanism of the generation, propagation and growth of dislocations in so-called dislocation-free silicon crystals. However, the results of the present work can definitely explain the fact that the dislocation generates from the bottom of the crystal, although only qualitatively.

## Conclusions

For silicon CZ crystal growth, a finite-element analysis of thermal stress in the crystal was carried out and the effect of a radiation shield inserted into the furnace on the thermal stress distribution was investigated theoretically. The following conclusions were obtained.

- (1) A non-flat melt/crystal interface is one of the major reasons for the incipience of dislocations from the bottom of a crystal, incidentally encountered during industrial single crystal growth.
- (2) A radiation shield can reduce the maximum shear stress, and there is an optimum location of the shield.
- (3) Maximum shear stress becomes larger as the Peclet number, i.e. the pulling rate, increases. From the viewpoint of thermal stress, a radiation shield allows a higher pull rate.

## Nomenclature

$A$	= matrix defined by Eq. (3)	[1/m]
$a$	= nodal displacement vector	[m]
$B$	= strain-nodal displacement matrix	[1/m]
$Cp_s$	= specific heat of crystal	[J/kg·K]
$D$	= elastic stress-strain matrix	[Pa]

$d$	= displacement vector	[m]
$E$	= Young's modulus	[Pa]
$k_l$	= thermal conductivity of melt	[W/m·K]
$Pe$	= Peclet number ( $= Cp_s V'_s r'_c / k_l$ )	[—]
$r'$	= radial distance in cylindrical coordinates	[m]
$r'_c$	= crucible radius	[m]
$r'_s$	= crystal radius	[m]
$r'_{sh}$	= radiation shield radius	[m]
$r, r_s, r_{sh}$	= $r'/r'_c, r'_s/r'_c, r'_{sh}/r'_c$	[—]
$T'$	= temperature	[K]
$u$	= radial component of displacement vector	[m]
$V'_m$	= melt volume	[m <sup>3</sup> ]
$V_m$	= $V'_m / 2\pi r_c'^3$	[—]
$V'_s$	= crystal pull rate	[m/s]
$v$	= axial component of displacement vector	[m]
$w'_{sh}$	= radiation shield width	[m]
$w_{sh}$	= $w'_{sh}/r'_c$	[—]
$z'$	= axial distance in cylindrical coordinates	[m]
$z'_{sh}$	= distance between crucible bottom and lower end of radiation shield	[m]
$z, z_{sh}$	= $z'/r'_c, z'_{sh}/r'_c$	[—]
$\Delta z'$	= maximum arc height of melt/crystal interface	[m]
$\beta$	= linear thermal expansion coefficient	[1/K]
$\varepsilon$	= strain	[—]
$\varepsilon_0$	= initial strain	[—]
$\nu$	= Poisson's ratio	[—]
$\rho$	= density of crystal	[kg/m <sup>3</sup> ]
$\sigma$	= stress	[Pa]

$\sigma_1, \sigma_2, \sigma_3$	= principal stress	[Pa]
$\tau_{max}$	= maximum shear stress	[Pa]
$\phi$	= trial function	[—]

#### Literature Cited

- 1) Jordan, A. S. and R. Caruso and A. R. Von Neida: *The Bell System Tech. J.*, **59**, 593 (1980).
- 2) Huang, C. E., D. Elwell and R. S. Feigelson: *J. Crystal Growth*, **69**, 275 (1984).
- 3) Kobayashi, K. and T. Iwaki: *J. Crystal Growth*, **73**, 96 (1985).
- 4) Lambropoulos, J. C.: *J. Crystal Growth*, **80**, 245 (1987).
- 5) Lambropoulos, J. C.: *J. Crystal Growth*, **84**, 349 (1987).
- 6) Lambropoulos, J. C. and C. N. Delametter: *J. Crystal Growth*, **92**, 390 (1988).
- 7) Motakef, S. and A. F. Witt: *J. Crystal Growth*, **80**, 37 (1987).
- 8) Motakef, S.: *J. Crystal Growth*, **88**, 341 (1988).
- 9) Schvezov, C., I. V. Samarasekera and F. Weinberg: *J. Crystal Growth*, **84**, 219 (1987).
- 10) Schvezov, C., I. V. Samarasekera and F. Weinberg: *J. Crystal Growth*, **85**, 142 (1987).
- 11) Szabo, G.: *J. Crystal Growth*, **73**, 131 (1985).
- 12) Touloukian, Y. S., R. K. Kirby, R. E., Taylor and P. D. Desai: *Thermophysical Properties of Matter*, vol. 12, IFI/PLENUM, New York, 1975.
- 13) Tsukada, T., N. Imaishi, M. Hozawa and K. Fujinawa: *J. Chem. Eng. Japan*, **20**, 146 (1987).
- 14) Tsukada, T., N. Imaishi and M. Hozawa: *J. Chem. Eng. Japan*, **21**, 381 (1988).